Stem Cell Reports
Article

ISSCR

OPEN ACCESS

MIF Plays a Key Role in Regulating Tissue-Specific Chondro-Osteogenic Differentiation Fate of Human Cartilage Endplate Stem Cells under Hypoxia

Yuan Yao,[1] Qiyue Deng,[2] Weilin Song,[3] Huiyu Zhang,[4] Yuanjing Li,[5] Yang Yang,[6] Xin Fan,[1] Minghan Liu,[1] Jin Shang,[1] Chao Sun,[1] Yu Tang,[1] Xiangting Jin,[7] Huan Liu,[1,*] Bo Huang,[1,*] and Yue Zhou[1,*]

[1]Department of Orthopedics, Xinqiao Hospital, Third Military Medical University, Chongqing 400037, China
[2]Department of Neurobiology, College of Basic Medical Sciences, Third Military Medical University, Chongqing 400038, China
[3]Department of Ophthalmology, Southwest Hospital, Third Military Medical University, Chongqing 400038, China
[4]Department of Stomatology, Xinqiao Hospital, Third Military Medical University, Chongqing 400037, China
[5]Department of Orthopedics, General Hospital of Xizang Military Region of PLA, Lasa 850003, China
[6]Department of Cardiology, Daping Hospital, Third Military Medical University, Chongqing 400042, China
[7]Department of Orthopedics, The 422nd Hospital of PLA, Zhanjiang 524009, China
*Correspondence: happyzhou@vip.163.com (Y.Z.), bighuang2000@hotmail.com (B.H.), 20016040@163.com (H.L.)
http://dx.doi.org/10.1016/j.stemcr.2016.07.003

SUMMARY

Degenerative cartilage endplate (CEP) shows decreased chondrification and increased ossification. Cartilage endplate stem cells (CESCs), with the capacity for chondro-osteogenic differentiation, are responsible for CEP restoration. CEP is avascular and hypoxic, while the physiological hypoxia is disrupted in the degenerated CEP. Hypoxia promoted chondrogenesis but inhibited osteogenesis in CESCs. This tissue-specific differentiation fate of CESCs in response to hypoxia was physiologically significant with regard to CEP maintaining chondrification and refusing ossification. MIF, a downstream target of HIF1A, is involved in cartilage and bone metabolisms, although little is known about its regulatory role in differentiation. In CESCs, MIF was identified as a key point through which HIF1A regulated the chondro-osteogenic differentiation. Unexpectedly, unlike the traditionally recognized mode, increased nuclear-expressed MIF under hypoxia was identified to act as a transcriptional regulator by interacting with the promoter of *SOX9* and *RUNX2*. This mode of HIF1A/MIF function may represent a target for CEP degeneration therapy.

INTRODUCTION

Degenerative disc disease (DDD) is considered to be the most important cause of low back pain (LBP), which is one of the most common reasons for activity limitation (Andersson, 1999). Many pathological factors account for DDD, such as cell senescence, inflammatory factors, and extracellular matrix degradation (Le Maitre et al., 2007; Peng et al., 2006; Wang et al., 2015). A declining metabolic exchange due to the accumulation of waste products and nutrition insufficiency appears to be the most important of these mechanisms (Buckwalter, 1995). The intervertebral disc (IVD) is the largest avascular organ in the human body, and the metabolic exchange is predominantly reliant on the diffusion effect across cartilage endplate (CEP) in the mature IVD (Holm et al., 1981). The CEP is a thin horizontal layer of hyaline cartilage that separates the IVD from the vertebral body. Blood vessels in the adjacent vertebral bones do not reach the inner component of the discs but end at the interface between IVD and the vertebrae (Raj, 2008). Because it is the most important metabolic exchange channel, many studies assert that the degeneration of CEP may initiate DDD (Li et al., 2010).

Chondrification characteristics are considered to be critical in the physiological function of CEP. Changes in the cartilaginous biochemical content of CEP are closely related to IVD degeneration. The matrix of CEP is primarily composed of collagen type II, which is not only necessary for cartilage to resist compressive forces but is also instrumental in the transport properties of CEP. In addition, CEP ossification reduces the solute transport, which finally leads to DDD (Roberts et al., 1996). However, the mechanisms responsible for the loss of chondrification and the onset of ossification remain unclear.

Recent studies by our group demonstrated the presence of stem cells in the CEP. These cartilage endplate stem cells (CESCs) exhibited superior capacity for chondrogenic and osteogenic differentiation to those of bone marrow mesenchymal stem cells (BM-MSCs) (Liu et al., 2011). This differentiation property attracted our attention because it is likely that CESCs play an important role in the restoration and regeneration of CEP, and the direction of chondrogenesis and osteogenesis in CESCs may be responsible for CEP chondrification and ossification.

As an avascular tissue, IVD remains in a hypoxic microenvironment (Boskey, 2008), and the oxygen tension within CEP is as low as 1% (Lee et al., 2007). Hypoxia greatly affects the chondrogenesis and osteogenesis of MSCs (Merceron et al., 2010), which indicates that physiological hypoxia may regulate the chondro-osteogenic differentiation of CESCs to maintain a balance of chondrification and ossification in CEP.

The hypoxia-inducible factor-1α subunit/macrophage migration inhibitory factor (HIF1A/MIF) pathway is one

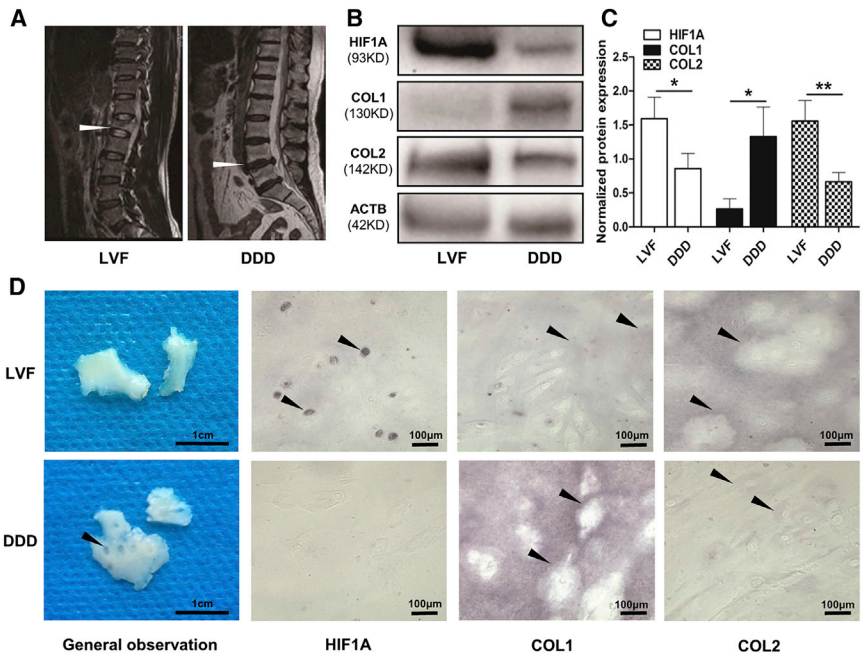

Figure 1. DDD CEP Exposed to Less Hypoxia Exhibited Less Chondrification and More Ossification than LVF CEP

(A) Representative MRI of patients. Patients with lumbar vertebral fracture (LVF) were classified as grade 1, and patients with lumbar DDD as grade 6 according to the Pfirrmann classification system. The arrowheads indicate the experimental material position.

(B and C) Western blot (B) and analysis (C) of the expressions of HIF1A, COL1, and COL2. Protein content was measured by densitometry and normalized according to ACTB level. The expressions of HIF1A and COL2 were decreased but the expression of COL1 was increased in DDD CEP compared with LVF CEP. Data represent the mean ± SD (n = 3 independent experiments, t test). *p < 0.05, **p < 0.01.

(D) General observation of samples and immunohistochemical staining in tissue sections. Arrowheads indicate small fissures in the DDD CEP, positively staining collagen matrix and positively staining cells.

of the most important signaling pathways in response to hypoxia. HIF1A is a key cellular regulator in responding to hypoxia; MIF, which has been recognized as a downstream target of HIF1A, acts as a regulator of innate immunity and can regulate many biological activities (Fu et al., 2010; Maity and Koumenis, 2006). MIF is highly involved in cartilage metabolism. *MIF* knockdown in zebrafish embryos can lead to undeveloped jaw cartilage (Ito et al., 2008). Moreover, MIF was observed to be involved in the degenerative process of CEP (Xiong et al., 2014). In mouse neural progenitor cells, MIF promoted survival and maintenance by upregulating the expression of SOX6, which is also a member of the SOX family and is co-expressed with SOX9 in all chondroprogenitors, indicating that MIF may initiate chondrogenesis in progenitor cells (Ohta et al., 2013). In addition, MIF was also involved in bone metabolism (Onodera et al., 2002). Transgenic mice overexpressing *MIF* exhibited osteoporosis, implying that the overexpression of *MIF* may lead to poor osteogenesis capability (Onodera et al., 2006). Obviously, the cartilage and bone metabolism was closely related to the chondrogenic and osteogenic differentiation of stem cells; however, the impact of the HIF1A/MIF pathway upon chondro-osteogenic differentiation is rarely reported. The transcription factor SOX9 is the master regulator of chondrogenesis and is expressed in pre-chondrocytes and differentiated chondrocytes during skeletal development (Healy et al., 1996). The transcription factor RUNX2 acts as the master regulator of skeletogenesis; its expression is necessary for osteoblast differentiation and maturation (Ducy et al., 1997). In this study, we investigated how the HIF1A/MIF pathway regulated *SOX9* and *RUNX2*, which resulted in a change in the chondro-osteogenic differentiation fate of CESCs.

RESULTS

Degenerated CEP under Relative Normoxia Lost Chondrification and Acquired Ossification

To understand changes in the chondrification, ossification, and hypoxic conditions during CEP degeneration, we assessed relatively normal CEP tissues in patients with lumbar vertebral fracture (LVF) without a formerly documented clinical history of LBP as the undegenerated group. We also assessed degenerated CEP tissues in patients with DDD as a degenerated group according to the Pfirrmann classification system (Pfirrmann et al., 2001) (Figure 1A). There were small fissures in the CEP samples of the degenerated group (Figure 1D). We then investigated the expression of HIF1A, collagen type I (COL1), and collagen type II (COL2) in human CEP from patients with LVF and DDD using western blot (Figures 1B and 1C) and immunohistochemistry (Figure 1D). The expression of HIF1A and COL2 was increased in CEP from LVF compared with those in CEP from DDD. Conversely, the expression of COL1 was remarkably decreased in CEP from LVF. These results showed that the degenerated CEP had lost chondrification and acquired ossification compared with the undegenerated group. In addition, HIF1A functioned as a sensor of

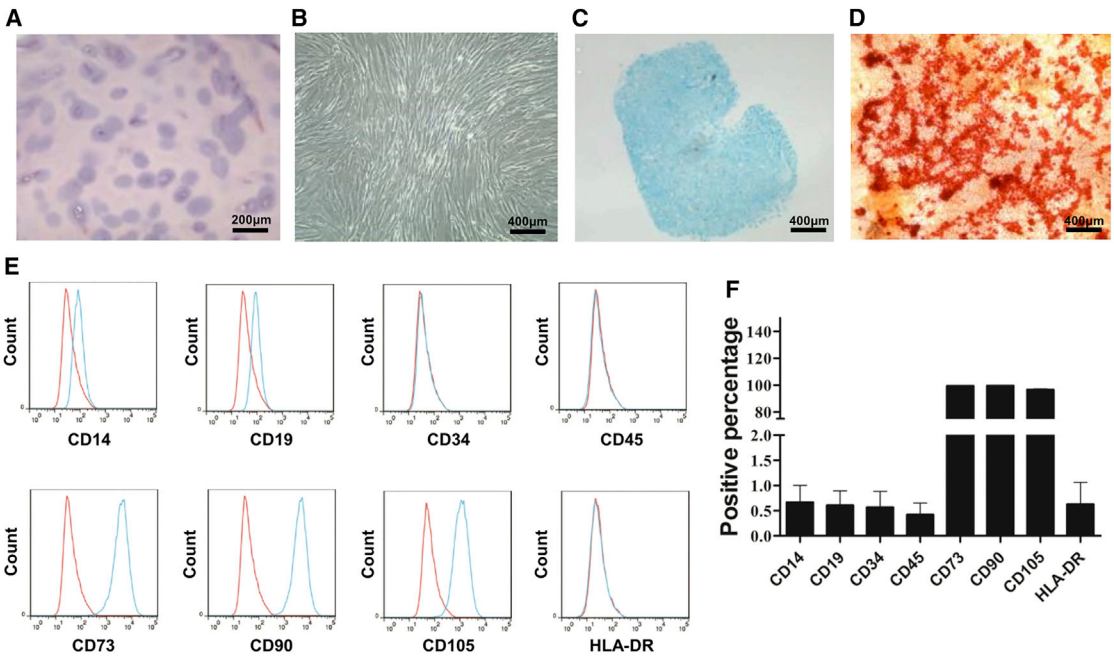

Figure 2. CESCs Shared Features with BM-MSCs Regarding Morphology, Stem Cell Surface Markers, and Differentiation Ability

(A) H&E staining of the tissue section.

(B) Morphology of CESCs in agarose after seeding 6 weeks later.

(C) Histologic section stained with Alcian blue of chondrified pellets in which CESCs formed in chondrogenic induction medium after 3 weeks.

(D) Alizarin red staining of CESCs that underwent osteogenic induction for 3 weeks.

(E) Immunophenotypic profile of stem cells in CESCs by flow cytometric analysis. The green lines indicate the fluorescence intensity of cells stained with the corresponding antibodies, and the red lines represent isotype-matched negative control cells.

(F) Percentages of CESCs expressing different stem cell markers (n = 6 independent experiments). Data represent the mean ± SD.

hypoxia, the robust expression of which was detected in avascular tissue such as the nucleus pulposus in IVD (Rajpurohit et al., 2002). The decreased expression of HIF1A suggested that the degenerated CEP remained in a less hypoxic microenvironment than the undegenerated CEP.

CESCs Exhibited Features Similar to Those of BM-MSCs

We used H&E staining to eliminate the possibility of pollution with other residual impurities (Figure 2A). CESCs exhibited a typical fibroblast-like morphology and a swirling-like pattern, which was homogeneous with BM-MSCs (Figure 2B). The multipotency of CESC differentiation was evaluated by induction into chondrogenic (Figure 2C) and osteogenic (Figure 2D) lineages in vitro. Cell-surface immunophenotypes were checked by flow cytometric analysis. Immunophenotypic evaluation showed that CESCs were positive for stem cell markers, including CD73, CD90, and CD105, but negative for CD14, CD19, CD34, CD45, and HLA-DR (Figures 2E and 2F), which met the criteria of the International Society for Cellular Therapy (Dominici et al., 2006).

HIF1A Promoted Chondrogenesis and MIF Expression while Inhibiting Osteogenesis

HIF1A is considered the master transcriptional regulator of cellular and developmental responses to hypoxia (Semenza, 2001). Dimethyloxalylglycine (DMOG), which increases the endogenous level of HIF1A, has been shown to mimic "chemical hypoxia" under normoxia. YC1, which downregulates HIF1A at posttranslational level, was used in our study to create "chemical normoxia" under hypoxia.

To evaluate the effect of HIF1A on chondrogenic differentiation and osteogenic differentiation in a hypoxic microenvironment, we induced CESCs in chondrogenic induction medium (CIM) and osteogenic induction medium (OIM) treated with PBS or DMOG under normoxia (21% O_2) and treated with PBS or YC1 under hypoxia (1% O_2).

The expression levels of SOX9 and COL2 in the normoxia + DMOG group and the hypoxia + PBS group were greater than those in the normoxia + PBS group both as mRNA (Figure 3A) and proteins (Figures 3B and 3C). Conversely, the expression levels of RUNX2 and COL1 in the normoxia + DMOG group and the hypoxia + PBS group

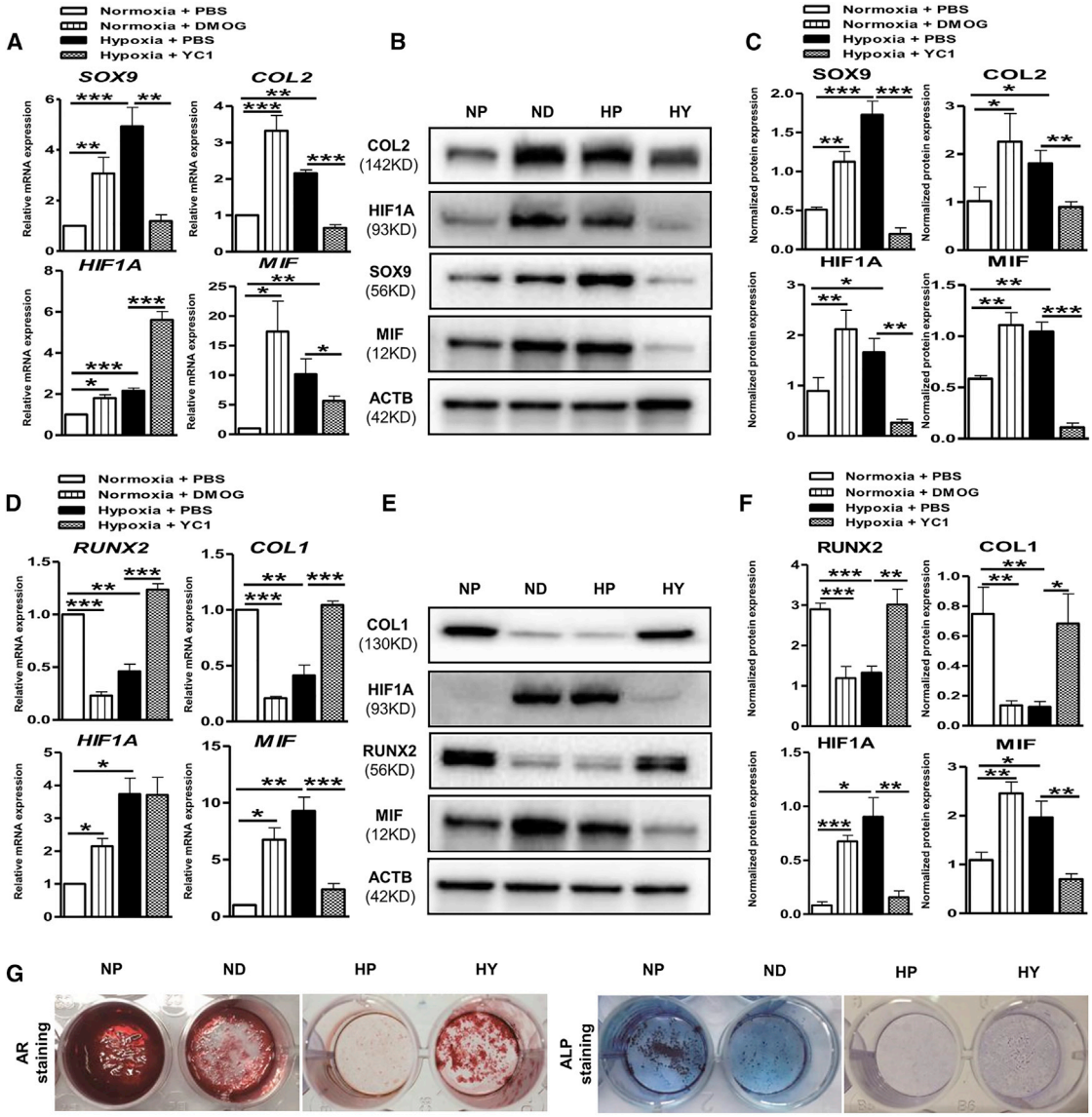

Figure 3. Hypoxia Increased Chondrogenic Differentiation and MIF Expression while Decreasing Osteogenic Differentiation by HIF1A

CESCs were induced under normoxia + PBS (NP), normoxia + DMOG (ND), hypoxia + PBS (HP), and hypoxia + YC1 (HY) conditions in chondrogenic induction medium (CIM) (A–C) or osteogenic induction medium (OIM) (D–G), respectively, for 3 weeks.

(A) Chondrogenic gene (*SOX9* and *COL2*), *HIF1A*, and *MIF* gene expression were assessed by RT-PCR of mRNA from CESCs induced in CIM.

(B and C) Western blot analysis of the expression of SOX9, COL2, HIF1A, and MIF in samples treated under the conditions in (A). The protein contents were normalized according to ACTB level.

(D) Osteogenic gene (*RUNX2* and *COL1*), *HIF1A*, and *MIF* gene expression were assessed by RT-PCR of mRNA from CESCs induced in OIM.

(E and F) Western blot analysis of the expression of RUNX2, COL1, HIF1A, and MIF in samples treated under the conditions in (D). The protein contents were normalized according to ACTB level.

(G) Macrographs of alizarin red staining and ALP staining of CESCs treated under the conditions in (D).

Data represent the mean ± SD (n = 3 independent experiments, t test). *p < 0.05, **p < 0.01, ***p < 0.001.

were significantly lower than those in the normoxia + PBS group both as mRNA (Figure 3D) and proteins (Figures 3E and 3F). After treatment with an HIF1A inhibitor (YC1) in a hypoxic microenvironment, the expressions of SOX9 and COL2 were markedly decreased (Figures 3A–3C), whereas the expression of RUNX2 and COL1 were

increased compared with those in the hypoxia + PBS group (Figures 3D–3F). HIF1A also had an inhibitory effect on the functional mineralization of CESCs (Figure 3G). These results revealed that HIF1A promoted chondrogenic differentiation and inhibited osteogenic differentiation in a hypoxic microenvironment.

After 21 days of induction, at the protein level the expressions of HIF1A in the normoxia + DMOG group and the hypoxia + PBS group were greater than those in the normoxia + PBS group, and the expression of HIF1A in the hypoxia + YC1 group was markedly decreased compared with that in the hypoxia + PBS group (Figures 3B, 3C, 3E, and 3F). These data implied that the method of treatment effectively regulated HIF1A. Notably, we observed that the expression of *HIF1A* at the mRNA level shared the same trend with that at the protein level under DMOG and hypoxia treatment, while under YC1 treatment, the mRNA level and the protein level of HIF1A expression exhibited a different trend. Thus YC1 might only regulate HIF1A at the posttranslational stage (Figures 3A and 3D).

Previous studies showed that MIF expression was increased in response to hypoxia (Fu et al., 2010). We initiated a study to investigate MIF regulation by hypoxia in CESCs. Our results indicated that, at both mRNA and protein levels, MIF was markedly increased when subjected to DMOG or hypoxia compared with normoxia; YC1-treated CESCs had significantly decreased MIF expression in response to hypoxia. These results provided evidence that MIF was a downstream target of HIF1A and that hypoxia induced MIF expression at both mRNA and protein levels from CESCs in an HIF1A-dependent manner.

MIF Was Responsible for HIF1A-Induced Chondro-Osteogenic Gene Expression under Hypoxia

To determine whether HIF1A-mediated MIF contributed to hypoxia-induced chondro-osteogenic changes, we designed short hairpin RNAs (shRNAs) against *MIF* and a lentiviral vector system to efficiently overexpress *MIF*. *MIF* shRNA and scrambled shRNA vector were applied to the normoxia + DMOG group and hypoxia + PBS group in which *MIF* expression should had been relatively high. *MIF* overexpression and scrambled overexpression vector were added to the normoxia + PBS group and hypoxia + YC1 group in which *MIF* expression should have been relatively low.

In CIM (Figures 4A–4C) and OIM (Figures 4D–4G), hypoxia and HIF1A upregulation mediated chondrogenesis and inhibited osteogenesis. This effect was reversed by shRNA against *MIF*. Normoxia and HIF1A downregulation mediated chondrogenesis. Osteogenesis was reversed by the overexpression of lentivirus against *MIF*.

As reported previously, MIF contributed to HIF stabilization by preventing proteasome-mediated degradation (Winner et al., 2007). There was a positive feedback loop between HIF1A and MIF (Gaber et al., 2011). These were confirmed in our experiment. At the protein level, we observed a near-complete rescue of HIF1A expression in *MIF* overexpression lentivirus-treated CESCs in a normoxia + PBS group or hypoxia + YC1 group (Figures 4B and 4C) and a nearly complete knockdown of HIF1A expression in *MIF*-shRNA-treated CESCs in a normoxia + DMOG group or hypoxia + PBS group (Figures 4E and 4F). At the transcription level, the change in *MIF* did not consistently influence the expression of *HIF1A*; changes in *MIF* varied according to the treatment system (Figures 4A and 4D). These data showed that MIF regulated HIF1A primarily on the protein level and not the mRNA level. These findings were consistent with previous research (Gaber et al., 2011).

MIF Expression Was Increased in the Cell Nucleus under Hypoxia

To detect the cellular location of MIF, we conducted an immunofluorescence analysis after induction. Unexpectedly, we observed that MIF expression in the nucleus was increased in the normoxia + DMOG and hypoxia + PBS groups compared with the normoxia + PBS and hypoxia + YC1 groups (Figures 5A and 5B). This phenomenon was confirmed by western blot analysis; the ratio of MIF expression in the nucleus compared with that in cytoplasm was greater in the normoxia + DMOG and hypoxia + PBS groups than in the normoxia + PBS and hypoxia + YC1 groups (Figures 5C and 5D). The change in the nuclear expression of MIF suggested of a dominant role of MIF in the cell nucleus.

MIF Promoted SOX9 Promoter Activity and Repressed RUNX2 Promoter Activity

Previous studies showed a unique contribution of MIF to the transcriptional regulation of some important transcriptional factors (Hudson et al., 1999; Petrenko et al., 2003; Petrenko and Moll, 2005). We observed that MIF was redistributed in the nucleus under hypoxia. We then sought to determine whether MIF played a role as a transcriptional regulator in regulating the transcriptional activities of two additional important transcription factors, *SOX9* and *RUNX2*.

To determine whether the transcriptional activities of *SOX9* and *RUNX2* were regulated by MIF during chondrogenesis and osteogenesis, we performed an analysis of promoter activities with luciferase reporter assay in a 293T cell line. We chose the putative regulatory loci of the *SOX9* and *RUNX2* genes (from −300 bp to 0 bp) according to previous studies (Colter et al., 2005; Hawse et al., 2011; Kanai and Koopman, 1999; Piera-Velazquez et al., 2007; Tamiya et al., 2008; Zhang et al., 2009). The

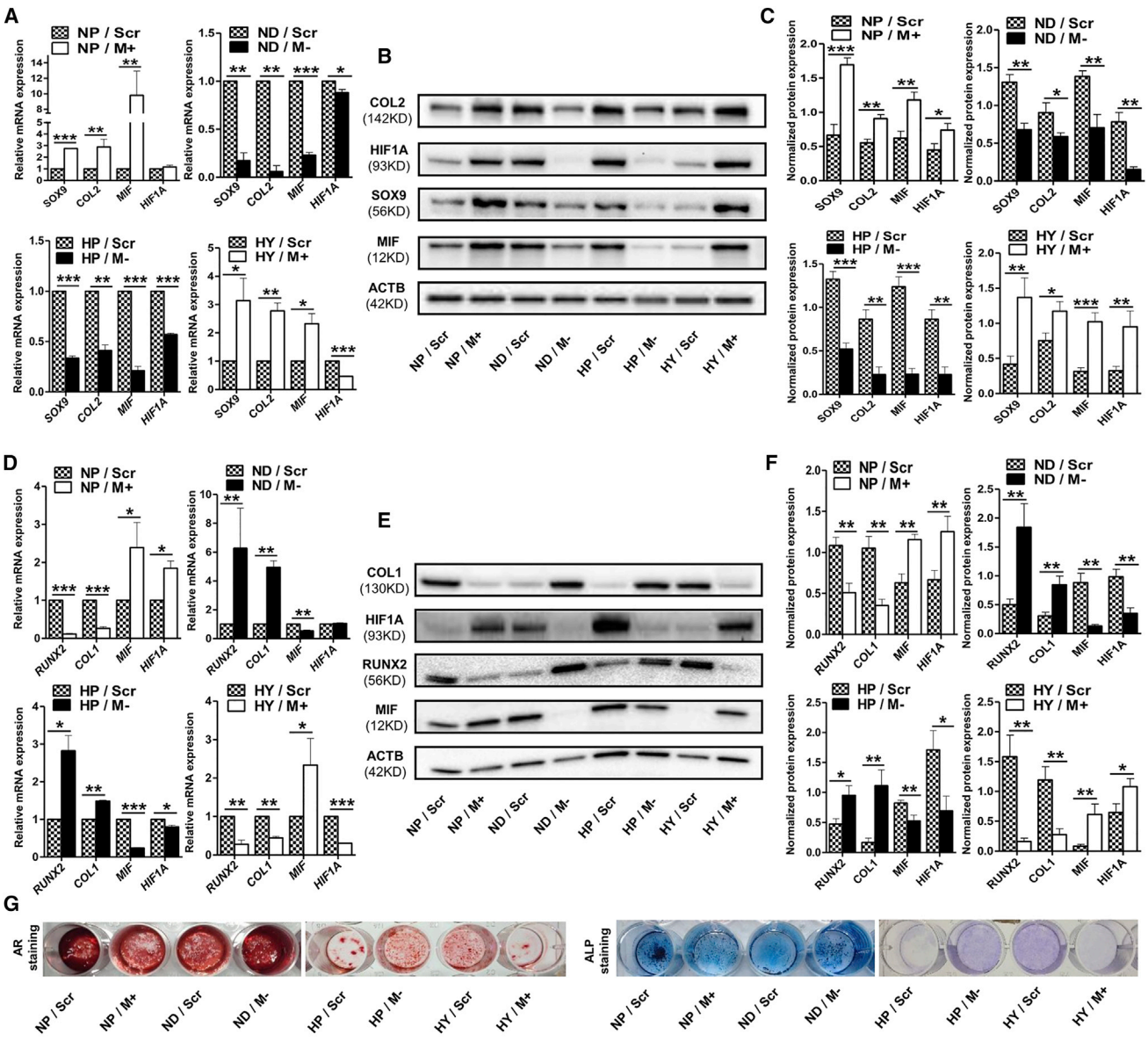

Figure 4. HIF1A Regulated Chondro-Osteogenic Differentiation of CESCs by MIF

CESCs assigned to normoxia + PBS (NP) and hypoxia + YC1 (HY) groups, in which *MIF* expression should have been relatively low, were transfected with *MIF*-overexpressing lentiviral vector system (M+) and its scramble control (Scr). CESCs assigned to normoxia + DMOG (ND) and hypoxia + PBS (HP) groups in which *MIF* expression should had been relatively high were transfected with *MIF*-shRNA (M−) and its scramble control (Scr).

(A) *SOX9*, *COL2*, *HIF1A*, and *MIF* gene expression were assessed by RT-PCR of mRNA from CESCs induced in CIM.

(B and C) Western blot analysis of the expression of SOX9, COL2, HIF1A, and MIF in samples treated under the conditions in (A).

(D) *RUNX2*, *COL1*, *HIF1A*, and *MIF* gene expression were assessed by RT-PCR of mRNA from CESCs induced in OIM.

(E and F) Western blot analysis of the expression of RUNX2, COL1, HIF1A, and MIF in the samples treated under the conditions in (D).

(G) Macrographs of alizarin red staining and ALP staining of CESCs treated under the conditions in (D).

Data represent the mean ± SD (n = 3 independent experiments, t test). *p < 0.05, **p < 0.01, ***p < 0.001.

upregulation of *SOX9* and the downregulation of *RUNX2* upon *MIF* overexpression could be due to the acquisition of transcriptional regulation by MIF (Figure 6A).

To determine whether MIF was associated with the promoter of *SOX9* and *RUNX2* via interaction with the recognizing region demonstrated via luciferase reporter assay, we

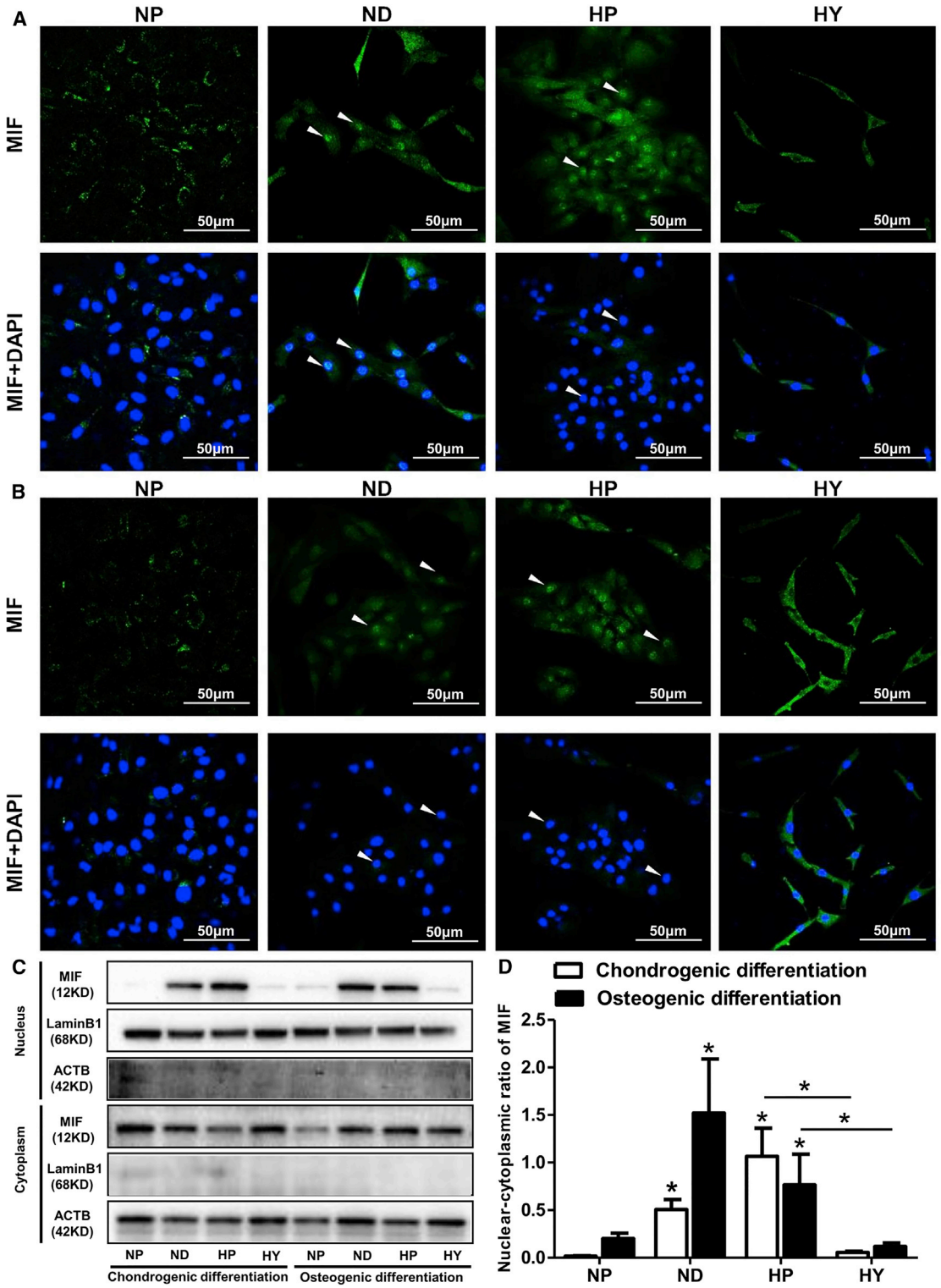

Figure 5. MIF Expression Was Increased in the Cell Nucleus under Hypoxia

(A and B) Immunofluorescence staining of CESCs under normoxia + PBS (NP), normoxia + DMOG (ND), hypoxia + PBS (HP), and hypoxia + YC1 (HY) conditions, respectively, in CIM (A) and OIM (B) for 3 weeks. Arrowheads indicate the nuclear MIF expression.

(legend continued on next page)

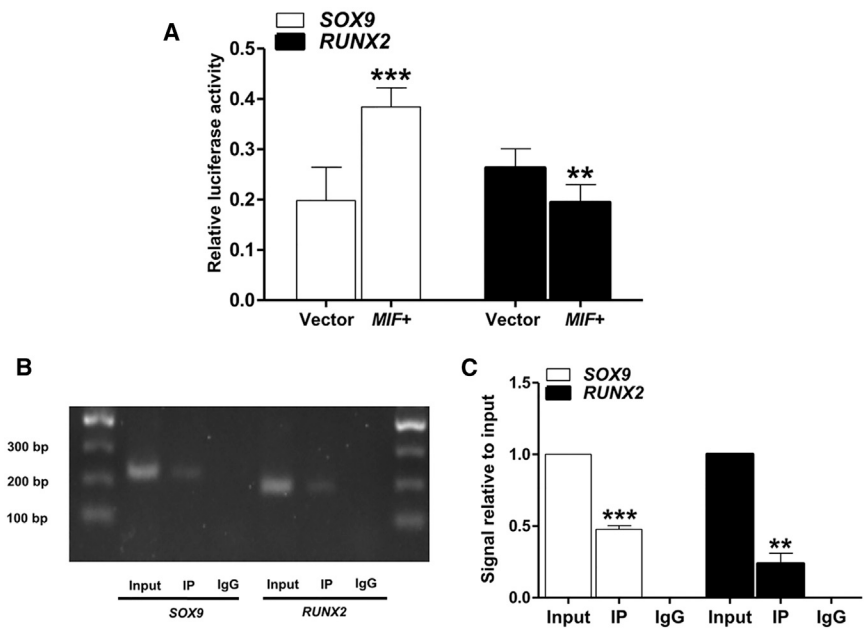

Figure 6. MIF Regulated the Transcription of *SOX9* and *RUNX2* by Interacting with the Promoters

(A) A luciferase reporter assay showed that overexpressing *MIF* regulated *SOX9* and *RUNX2* promoter activities. Reporter constructs containing −300 bp to 0 bp were constructed (n = 3 independent experiments, t test).

(B and C) ChIP analysis of CESCs. The extracted chromatins were incubated with anti-MIF antibody or isotype IgG antibody. A 231-bp fragment in the −300 bp to 0 bp region in the *SOX9* promoter and a 195-bp fragment in the −300 bp to 0 bp region in the *RUNX2* promoter were amplified by PCR (B) and qRT-PCR (C). The results were normalized to the input control (n = 3 independent experiments, t test).

Data represent the mean ± SD. **p < 0.01, ***p < 0.001.

performed a chromatin immunoprecipitation (ChIP)-PCR assay using CESCs. PCR amplification (Figure 6B) and real-time PCR (Figure 6C) showed that a 231-bp DNA fragment corresponding to a sequence from −291 bp to −61 bp in the *SOX9* promoter region and a 195-bp DNA fragment corresponding to a sequence from −288 bp to −94 bp in the *RUNX2* promoter region were immunoprecipitated with MIF antibody in CESCs. Figure 7 is a schematic diagram of proposed mechanisms for HIF1A/MIF-mediated regulatory effects on chondro-osteogenic differentiation in CESCs.

DISCUSSION

The CEP arises from embryonic mesoderm-derived tissue, and CESCs share characteristics related to cell-surface immunophenotype and the capacity to differentiate into mesoderm-derived cells, namely osteocytes, chondroblasts, and adipocytes (Liu et al., 2011), CESCs are thus considered as MSCs.

Common sources of MSCs in studies usually exist under hypoxic conditions: bone marrow (4%–7%), adipose tissue (3.8%–9.6%), and muscle tissue (1%–10%) (D'Ippolito et al., 2006; Redshaw and Loughna, 2012; Schiller et al., 2013). The tissue specificity of the differentiation of the MSCs in response to hypoxia can be observed. In BM-MSCs, hypoxia promoted chondrogenesis and inhibited osteogenesis and adipogenesis (Khan et al., 2010; Martin-Rendon et al., 2007; Yang et al., 2011). Adipose-derived MSCs tended to differentiate into adipocytes or chondrocytes, and the ability of osteogenic differentiation was dwarfed under hypoxia (Kim et al., 2014; Merceron et al., 2010). In muscle stem cells, low oxygen concentration favored myogenic differentiation but suppressed adipogenic differentiation (Redshaw and Loughna, 2012). The periodontal ligament stem cells promoted osteogenic differentiation under hypoxia (Zhang et al., 2014). Taken together, stem cells from different tissues show different tissue-specific differentiation fate in the physiological hypoxic microenvironment, which may facilitate the restoration and regeneration function of stem cells.

To determine tissue specificity in CESC differentiation, we performed chondrogenic and osteogenic induction under normoxia and hypoxia, respectively. Our study revealed tissue specificity indicating that hypoxia promoted chondrogenesis but inhibited osteogenesis in CESCs. This tissue specificity of CESC differentiation in response to physiological hypoxia contributed to our understanding of the mechanism of CEP degeneration in the context of CESCs. Due to the avascular nature, in CEP the oxygen tension was as low as 1% (Lee et al., 2007). As previous studies

(C) Western blot of the nuclear MIF expression (upper panels) and cytoplasmic MIF expression (lower panels) in CIM and OIM. The nuclear and cytoplasmic protein expressions were normalized by LaminB1 and ACTB, respectively.

(D) Nuclear-cytoplasmic ratio of MIF, the quantitative analysis of (C). Data represent the mean ± SD (n = 3 independent experiments, t test). *p < 0.05.

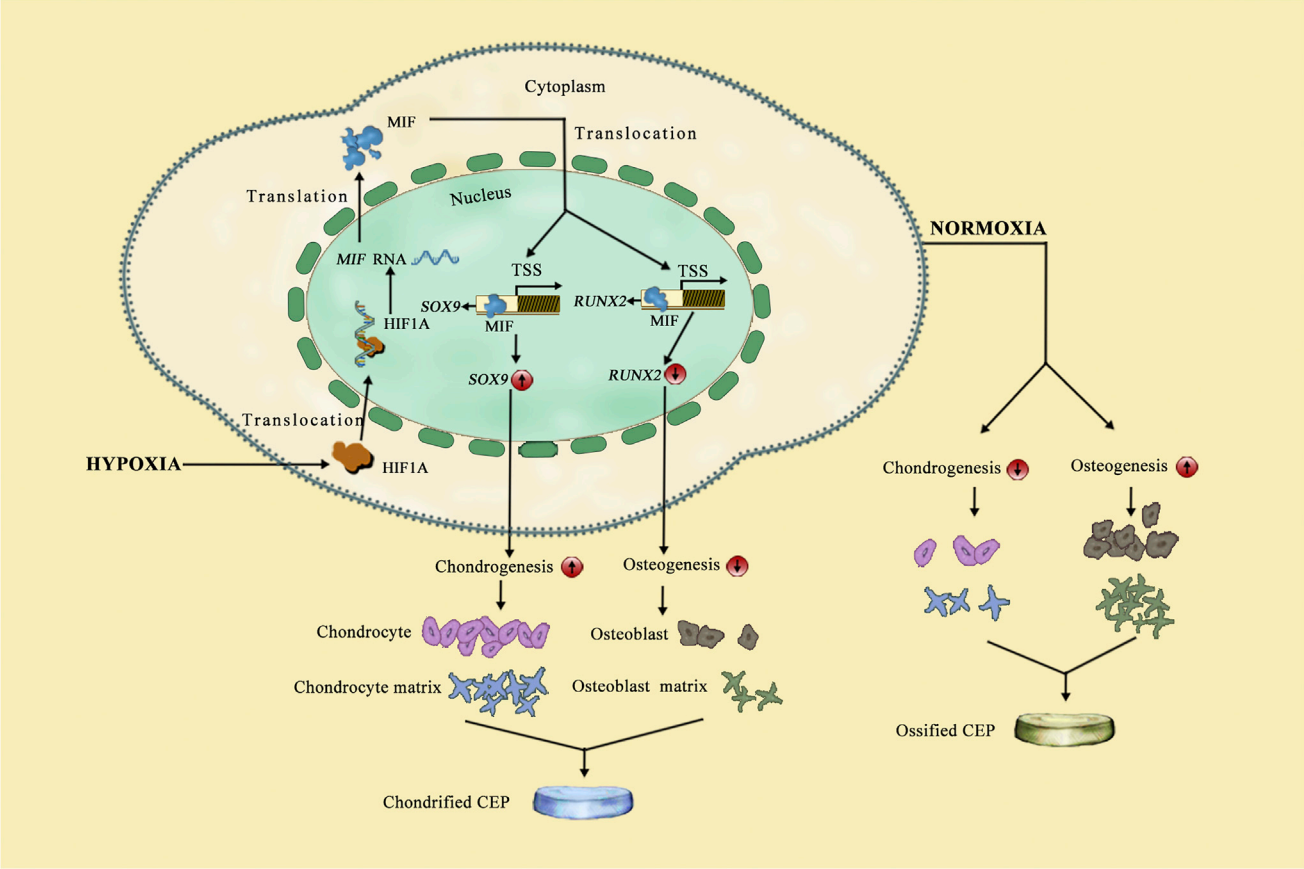

Figure 7. Schematic Diagram of Proposed Mechanisms for HIF1A/MIF-Mediated Regulatory Effects on Chondro-Osteogenic Differentiation in CESCs

TSS, transcription start site.

described, the CEP was free of blood vessels in groups of healthy juveniles and adolescents without a history of LBP. In adults and seniors with DDD, there were defects in the CEP whereby blood vessel invasion could be observed (Nerlich et al., 2007). Blood vessel invasion was also noted in painful human IVD (Freemont et al., 2002). In osteoarthritis, osteochondral angiogenesis within subchondral spaces was often caused by the invasion of neovessels that increased the oxygen level (Walsh et al., 2010). It is reasonable to assert that, in degenerated CEP, blood vessel invasion through small fissures accompanied by an increased oxygen tension in the microenvironment could disrupt the physiological hypoxic microenvironment of CESCs. This destruction could inhibit CESCs chondrogenic differentiation and facilitate osteogenic differentiation, which could initiate the loss of chondrification and the acquisition of ossification in CEP. The ossification of CEP resulted in a poor capacity to resist mechanical stress and poor nutrient exchange; complete IVD degeneration was thus initiated.

In a study of chondro-osteogenic differentiation in CESCs, we observed a critical role of HIF1A in regulating the direction of differentiation. HIF1A was a key cellular regulator in responding to a low oxygen level (Coimbra et al., 2004). A number of cartilage-related and osteogenesis-related genes were under transcriptional control by HIF1A (Robins et al., 2005; Wagegg et al., 2012). Given this background, we mimicked "chemical hypoxia" under normoxia via DMOG upregulating the expression of HIF1A and "chemical normoxia" under hypoxia by YC1 downregulating the expression of HIF1A. We observed that the promotion of chondrogenesis and the inhibition of osteogenesis were directly correlated with the expression of HIF1A in CESCs.

We then investigated how HIF1A regulated chondrogenesis and osteogenesis. A cytokine, MIF, which had been recognized as an important hypoxia-induced gene, was a downstream target of HIF1A. MIF acted as a regulator of innate immunity and could regulate many biological activities, such as cell proliferation, senescence, and angiogenesis. Notably, although MIF was involved in cartilage

and bone metabolism, the regulation of chondro-osteogenic differentiation by MIF has not been studied. In CESCs, we observed that MIF acted as a key factor in chondro-osteogenic differentiation under hypoxia. Firstly, consistent with previous research, MIF expression was induced by hypoxia at the level of mRNA and protein in an HIF1A-dependent manner. Secondly, hypoxia and HIF1A mediated changes in the ability of chondro-osteogenesis to be reversed by MIF expression via human intervention.

The mode of action of MIF in previous studies can be encapsulated in five aspects: (1) MIF receptor, (2) activation of ERK1/ERK2, (3) upregulation of TLR4 expression, (4) suppression of p53 activity, and (5) inhibition of JAB1 activity (Calandra and Roger, 2003; Lue et al., 2002). We next investigated the presence of other pathways. Unexpectedly, in CESCs an increased nuclear MIF expression under hypoxia was observed. As previous studies described, a high nuclear expression of MIF could also be observed in the tissues of lung adenocarcinoma, glioblastoma multiforme, pituitary adenoma, and aggressive bladder cancer (Kamimura et al., 2000; Markert et al., 2001; Pyle et al., 2003; Taylor et al., 2007); the same was observed in our study using CESCs. Tumor tissue is very hypoxic, and we speculated that increased nuclear MIF expression may occur in this hypoxic microenvironment. MIF may not act in the traditional manner but may play a biological role in the nucleus. After the analysis of the three-dimensional structure of MIF, we considered that MIF might lack a typical DNA-binding motif. In this study, ChIP showed the potential interaction between MIF and the promoter regions of *SOX9* and *RUNX2*, leading us to conclude that MIF could bind to DNA indirectly via intermediate proteins. From the result of the luciferase report, we observed that MIF could participate in the regulation of transcription. Based on the above information, we think that MIF could act as a "transcriptional regulator" that participates in the regulation of transcription indirectly, but not as a "transcription factor" that functions via direct binding to DNA sequences. A limitation of this study is that the intermediate mechanism has not been fully investigated. Further studies are required to illuminate this mechanism.

Noticeably, the redistribution of protein from the cytoplasm to the nucleus was observed in many regulatory molecules, such as nuclear factor κB (Haddad, 2009) and AKT (Xuan et al., 2006). We thus speculated that the increased nuclear MIF in hypoxic tumors may interact with the transcription factors responsible for cell growth, apoptosis, and angiogenesis in a manner similar to that of MIF regulating *SOX9* and *RUNX2* in CESCs.

In conclusion, this work firstly explained the clinical pathological phenomenon by which degenerative CEP decreased chondrification and increased ossification. The change in the differentiation fate of CESCs in response to disrupted physiological hypoxia could represent the cytological basis of CEP degeneration, which would initiate the degeneration of the entire IVD at a later stage. The maintenance of tissue specificity in stem cells depended on a subtle balance in the microenvironment, whereby some key cytokines played decisive roles in determining the function of stem cells. In CEP, the differentiation fate of CESCs was determined by the hypoxic microenvironment. Secondly, the study showed that MIF exhibited an important regulating function in the chondro-osteogenic differentiation fate of stem cells. Thirdly, unlike the traditionally recognized mode, a regulatory HIF1A/MIF pathway in which MIF acted as a transcriptional regulator in the nucleus was observed in CESCs under hypoxia, which represents an attractive target for therapeutic modalities to treat degeneration. In addition, the HIF1A/MIF pathway played crucial roles in cell proliferation (Gaber et al., 2011), senescence (Maity and Koumenis, 2006) and angiogenesis (Chesney et al., 1999) in the hypoxic tissue, especially in tumors. Whether these biological processes were also regulated by this mode warrants further study.

EXPERIMENTAL PROCEDURES

Patients and Subjects

The CEP tissues used in this study were obtained from patients who underwent discectomy and fusion operations at the Xinqiao Hospital of the Third Military Medical University (see also Table S1). The relatively normal human CEP control tissues were obtained from three patients with LVF without a history of LBP. The degenerated CEP were obtained from six patients with DDD. The state of IVD degeneration was evaluated according to the Pfirrmann classification system (Pfirrmann et al., 2001). The study procedures were approved by the Ethics Committee of Xinqiao Hospital, Third Military Medical University and were in accordance with the Helsinki Declaration, and written informed consent was obtained from each patient.

Lentivirus

MIF shRNA lentiviral particles (Santa Cruz Biotechnology, sc-37137-V) and scrambled shRNA lentiviral particles (Santa Cruz, sc-108080) were purchased for the knockdown of MIF expression (accession no. Genbank: NM_002415.1). *MIF* overexpression lentivirus (on vector pLenti6.3_MCS_IRES2-EGFP, Invitrogen) and a scrambled vector were packed by Invitrogen.

Tissue Procurement

The surgically explanted CEP were cleaned of any adherent tissues and washed with 0.1 M sterile PBS. A small portion of CEP tissue was saved for H&E staining to eliminate the possibility of pollution of any other residual impurity.

Immunohistochemistry and Histology

The CEP specimens were freshly collected in the operating room, fixed immediately in 4% formalin for 12 hr, and dehydrated

through 40% sucrose solutions for 48 hr. Sections were cut to 5-μm thickness, put onto glass slides, and dried for 3 hr. The slides for staining were blocked for endogenous peroxidase activity using 3% H_2O_2 solution for 5 min. They were then blocked with 3% goat serum, incubated in rabbit anti-human HIF1A antibody (Abcam, ab85886), mouse anti-human COL1 antibody (Abcam, ab90395), and rabbit anti-human COL2 antibody (Abcam, ab34712), respectively, overnight at 4°C, washed three times in PBS, and incubated in the corresponding secondary antibody (anti-rabbit immunoglobulin-horseradish peroxidase [IgG-HRP]-linked antibody, Cell Signaling Technology, #7074; anti-mouse IgG-HRP-linked antibody, Cell Signaling, #7076) for 1 hr with washing three times in PBS. Immunoreactive proteins were revealed with nickel-diaminobenzidine. Images were obtained with a microscope.

CESC Isolation and Culture

The CEP samples were mechanically minced and digested with 0.2% collagenase II (Sigma-Aldrich) in DMEM/F12 medium (Hyclone) containing 1% fetal calf serum (FCS; Gibco) for 12 hr at 37°C. The suspended cells were then filtered through a 70-μm cell filter. The suspension was centrifuged for 5 min at 1,000 rpm/min. After removing the suspension solution, the pellet was resuspended with culture medium containing DMEM/F12, 10% FCS, and 1% penicillin-streptomycin (Hyclone). Finally, the cells were cultured in a 25-cm^2 cell-culture flask at 37°C and 5% CO_2 condition. After the first passage of expansion, cells were cultured in agarose solution. The agarose selection system was established as previously described (Liu et al., 2011). In brief, culture dishes were coated with 1% low-melting-point agarose (Invitrogen). Then a mixture of 0.5 mL of DMEM/F12 medium, 0.5 mL of 2% low-melting-point agarose, and 1 mL of culture medium with 5×10^4 CEP cells was added to the culture dishes. The culture dishes were then transferred in a humidified atmosphere with 5% CO_2 at 37°C. The culture medium was changed twice per week. After 6 weeks, cell aggregates were aspirated with a sterile Pasteur pipette and cultured in a 25-cm^2 cell-culture flask. Passage 3 cells were used in this study.

Flow Cytometry

CESCs were trypsinized and washed in PBS and stained with the following conjugated antibodies: mouse anti-human CD14-FITC (eBioscience, 11-0149-41), mouse anti-human CD19-FITC (eBioscience, 11-0199-41), mouse anti-human CD34-FITC (eBioscience, 11-0349-41), mouse anti-human CD45-FITC (eBioscience, 11-9459-41), mouse anti-human CD73-FITC (eBioscience, 11-0739-41), mouse anti-human CD90-FITC (eBioscience, 11-0909-41), mouse anti-human CD105-PE (eBioscience, 12-1057-41), mouse anti-human HLA-DR-PerCP-Cyanine 5.5 (eBioscience, 45-9956-41). IgG (mouse IgG1 kappa isotype control-FITC, eBioscience, 11-4714-81; mouse IgG1 kappa isotype control-PE, eBioscience, 12-4714-41; mouse IgG2b kappa isotype control-PerCP-Cyanine 5.5, eBioscience, 45-4732-80) were used as isotype control. The final antibody concentration was at 1 mg/200 mL. After incubating for 30 min at 37°C, the cells were washed three times with PBS. Finally, labeled CESCs were subjected to flow cytometry analysis, and the percentage of positive staining was calculated relative to the isotype control staining.

Induction and Oxygen Deprivation

For chondrogenic or osteogenic differentiation, cells were induced in CIM (Cyagen) or OIM (Cyagen). For hypoxic culture, CESCs were cultured in a 1% O_2 condition or treated in medium containing 100 μM HIF1A inducer (DMOG; Sigma-Aldrich) in normoxic conditions (21% O_2). For normoxic culture, CESCs were cultured in normoxic conditions (21% O_2) or treated in medium containing 100 μM HIF1A inhibitor (YC1; Sigma-Aldrich) in hypoxic conditions (1% O_2). The induction medium was changed twice per week over a 21-day period.

Alizarin Red and ALP Staining

For identification of the mineral deposits after OIM induction, cells were fixed for 30 min with 4% paraformaldehyde (PFA), washed three times in PBS, and stained with alizarin red (Cyagen) for 5 min and then washed three times in PBS. For alkaline phosphatase (ALP) staining, the cells were fixed with 4% PFA for 30 min and stained with an alkaline phosphatase assay kit (Beyotime) according to the manufacturer's instructions, then washed three times with PBS. The stained cultures were photographed.

qRT-PCR

RNA was purified via Trizol extraction (Invitrogen). The RNA was transcribed into cDNA with a PrimeScript RT Master Mix Kit (TaKaRa). The primers were designed to amplify 100–250-bp-sized products (see also Table S2). The ABI 7900H Real-Time PCR system and the SYBR Premix Ex Taq II (TaKaRa) were used for qRT-PCR. The qPCR reactions were incubated at 95°C for 30 s followed by 40 cycles of 95°C for 5 s and 60°C for 34 s and a dissociation curve analysis. The expressions of each gene were normalized to *Actin-beta* (*ACTB*) expression.

Western Blot

Western cell lysis buffer (Beyotime) was used for the extraction of total protein. Nuclear and cytoplasmic protein extraction kits (Beyotime) were used for the extraction of nuclear and cytoplasmic proteins, respectively. Protein extraction was performed according to the manufacturer's instructions. Protein concentration was determined using the BCA kit (Beyotime). Approximately 30 μg of protein from each sample was diluted in PBS and 5× loading buffer was boiled for 5 min, separated via SDS-PAGE (Willget Biotech), and transferred to a polyvinylidene fluoride membrane (Bio-Rad). The tailored membranes were incubated with the corresponding primary antibodies (rabbit anti-human ACTB, Abcam, ab8227; rabbit anti-human anti-LaminB1, Abcam, ab65986; rabbit anti-human SOX9, Abcam, ab3697; rabbit anti-human COL2, Abcam, ab34712; rabbit anti-human RUNX2, Cell Signaling, #12556; mouse anti-human COL1, Abcam, ab90395; rabbit anti-human HIF1A, Abcam, ab85886; rabbit anti-human MIF, Abcam, ab175189), respectively, overnight at 4°C, washed three times in PBS, and incubated in the corresponding secondary antibody (anti-rabbit IgG-HRP-linked antibody, Cell Signaling, #7074; anti-mouse IgG-HRP-linked antibody, Cell Signaling, #7076) for 1 hr with washing three times in PBS, then subjected to western blotting using a Pierce ECL western blotting substrate kit (Thermo Scientific). Immunoreactive proteins were measured by chemiluminescent detection. The expressions of proteins were normalized to the ACTB level.

Immunofluorescence

Cells were reseeded in cell-culture dishes. After induction, the cells were fixed in 4% PFA and treated with a blocking solution containing 1% goat serum and 0.5% Triton X-100. The cells were stained with rabbit anti-human MIF antibody (Abcam, ab175189) overnight at 4°C. The cells were then washed three times with PBS and incubated with FITC-conjugated goat anti-rabbit IgG secondary antibody (Invitrogen, A24532) for 1 hr at room temperature. Subsequently, cell nuclei were stained with 0.1 mg/mL DAPI (Invitrogen). The stained cells were examined with a confocal microscope.

Luciferase Assay

Genomic DNA from 293T cells was used to amplify the −300 bp to 0 bp fragment of the human *SOX9* and *RUNX2* promoter region, which was cloned into the pGL3-basic vector (Promega) using HindIII and SmaI sites (primers listed in Table S2). The reporter gene constructs were co-transfected into 293T cells with *MIF*-overexpressing plasmids and scramble control plasmids using Lipofectamine 2000 reagent (Invitrogen). Renilla luciferase plasmid (Promega) was used as a normalized control with Lipofectamine 2000. Firefly and Renilla luciferase activities were measured consecutively with the dual luciferase assay kit (Promega) 48 hr after transfection.

Chromatin Immunoprecipitation

CESCs were crosslinked with 1% formaldehyde for 20 min at 37°C and sonicated. The DNA-protein mixture was then isolated with a ChIP assay kit (Millipore) according to the manufacturer's instructions with rabbit anti-human MIF antibody (Abcam, ab175189). The precipitated DNA was quantified using RT-PCR with primers listed in Table S2. The results were normalized according to the input control.

Statistical Analyses

The data are expressed as the mean ± SD of independent experiments. Comparisons were made using independent-samples t tests when comparing two experimental groups. Significance values were set at a p value of <0.05.

SUPPLEMENTAL INFORMATION

Supplemental Information includes two tables and can be found with this article online at http://dx.doi.org/10.1016/j.stemcr.2016.07.003.

AUTHOR CONTRIBUTIONS

Y.Z., B.H., and H.L. oversaw the study. Y. Yao, Q.D., Y.L., Y. Yang, H.Z., X.F., M.L., C.S., and J.S. conducted the experiments. Y. Yao, W.S., and Y.T. analyzed the data. Y. Yao and X.J. wrote the manuscript.

ACKNOWLEDGMENTS

We thank Y. Wang for providing the schematic diagram. This work was supported by the National Natural Science Foundation of China (No. 81472076, No. 81271982, No. 81401801, and No. 81572186).

Received: April 8, 2016
Revised: July 6, 2016
Accepted: July 6, 2016
Published: August 9, 2016

REFERENCES

Andersson, G.B. (1999). Epidemiological features of chronic low-back pain. Lancet *354*, 581–585.

Boskey, A.L. (2008). Signaling in response to hypoxia and normoxia in the intervertebral disc. Arthritis Rheum. *58*, 3637–3639.

Buckwalter, J.A. (1995). Aging and degeneration of the human intervertebral disc. Spine (Phila Pa 1976) *20*, 1307–1314.

Calandra, T., and Roger, T. (2003). Macrophage migration inhibitory factor: a regulator of innate immunity. Nat. Rev. Immunol. *3*, 791–800.

Chesney, J., Metz, C., Bacher, M., Peng, T., Meinhardt, A., and Bucala, R. (1999). An essential role for macrophage migration inhibitory factor (MIF) in angiogenesis and the growth of a murine lymphoma. Mol. Med. *5*, 181–191.

Coimbra, I.B., Jimenez, S.A., Hawkins, D.F., Piera-Velazquez, S., and Stokes, D.G. (2004). Hypoxia inducible factor-1 alpha expression in human normal and osteoarthritic chondrocytes. Osteoarthritis Cartilage *12*, 336–345.

Colter, D.C., Piera-Velazquez, S., Hawkins, D.F., Whitecavage, M.K., Jimenez, S.A., and Stokes, D.G. (2005). Regulation of the human Sox9 promoter by the CCAAT-binding factor. Matrix Biol. *24*, 185–197.

D'Ippolito, G., Diabira, S., Howard, G.A., Roos, B.A., and Schiller, P.C. (2006). Low oxygen tension inhibits osteogenic differentiation and enhances stemness of human MIAMI cells. Bone *39*, 513–522.

Dominici, M., Le Blanc, K., Mueller, I., Slaper-Cortenbach, I., Marini, F., Krause, D., Deans, R., Keating, A., Prockop, D., and Horwitz, E. (2006). Minimal criteria for defining multipotent mesenchymal stromal cells. The International Society for Cellular Therapy position statement. Cytotherapy *8*, 315–317.

Ducy, P., Zhang, R., Geoffroy, V., Ridall, A.L., and Karsenty, G. (1997). Osf2/Cbfa1: a transcriptional activator of osteoblast differentiation. Cell *89*, 747–754.

Freemont, A.J., Watkins, A., Le Maitre, C., Baird, P., Jeziorska, M., Knight, M.T., Ross, E.R., O'Brien, J.P., and Hoyland, J.A. (2002). Nerve growth factor expression and innervation of the painful intervertebral disc. J. Pathol. *197*, 286–292.

Fu, H., Luo, F., Yang, L., Wu, W., and Liu, X. (2010). Hypoxia stimulates the expression of macrophage migration inhibitory factor in human vascular smooth muscle cells via HIF-1alpha dependent pathway. BMC Cell Biol. *11*, 66.

Gaber, T., Schellmann, S., Erekul, K.B., Fangradt, M., Tykwinska, K., Hahne, M., Maschmeyer, P., Wagegg, M., Stahn, C., Kolar, P., et al. (2011). Macrophage migration inhibitory factor counter-regulates dexamethasone-mediated suppression of hypoxia-inducible factor-1 alpha function and differentially influences human CD4+ T cell proliferation under hypoxia. J. Immunol. *186*, 764–774.

Haddad, J.J. (2009). Endotoxin-mediated regulation of nuclear factor-kappaB nuclear translocation and activation in the hippocampus of the central nervous system: modulation by intracerebroventricular treatment with thymulin and the immunomodulatory role of the IkappaB-alpha/pIkappaB-alpha pathway. Neuroscience *164*, 1509–1520.

Hawse, J.R., Cicek, M., Grygo, S.B., Bruinsma, E.S., Rajamannan, N.M., van Wijnen, A.J., Lian, J.B., Stein, G.S., Oursler, M.J., Subramaniam, M., et al. (2011). TIEG1/KLF10 modulates Runx2 expression and activity in osteoblasts. PLoS One *6*, e19429.

Healy, C., Uwanogho, D., and Sharpe, P.T. (1996). Expression of the chicken Sox9 gene marks the onset of cartilage differentiation. Ann. N. Y. Acad. Sci. *785*, 261–262.

Holm, S., Maroudas, A., Urban, J.P., Selstam, G., and Nachemson, A. (1981). Nutrition of the intervertebral disc: solute transport and metabolism. Connect. Tissue Res. *8*, 101–119.

Hudson, J.D., Shoaibi, M.A., Maestro, R., Carnero, A., Hannon, G.J., and Beach, D.H. (1999). A proinflammatory cytokine inhibits p53 tumor suppressor activity. J. Exp. Med. *190*, 1375–1382.

Ito, K., Yoshiura, Y., Ototake, M., and Nakanishi, T. (2008). Macrophage migration inhibitory factor (MIF) is essential for development of zebrafish, *Danio rerio*. Dev. Comp. Immunol. *32*, 664–672.

Kamimura, A., Kamachi, M., Nishihira, J., Ogura, S., Isobe, H., Dosaka-Akita, H., Ogata, A., Shindoh, M., Ohbuchi, T., and Kawakami, Y. (2000). Intracellular distribution of macrophage migration inhibitory factor predicts the prognosis of patients with adenocarcinoma of the lung. Cancer *89*, 334–341.

Kanai, Y., and Koopman, P. (1999). Structural and functional characterization of the mouse Sox9 promoter: implications for campomelic dysplasia. Hum. Mol. Genet. *8*, 691–696.

Khan, W.S., Adesida, A.B., Tew, S.R., Lowe, E.T., and Hardingham, T.E. (2010). Bone marrow-derived mesenchymal stem cells express the pericyte marker 3G5 in culture and show enhanced chondrogenesis in hypoxic conditions. J. Orthop. Res. *28*, 834–840.

Kim, J.H., Kim, S.H., Song, S.Y., Kim, W.S., Song, S.U., Yi, T., Jeon, M.S., Chung, H.M., Xia, Y., and Sung, J.H. (2014). Hypoxia induces adipocyte differentiation of adipose-derived stem cells by triggering reactive oxygen species generation. Cell Biol. Int. *38*, 32–40.

Le Maitre, C.L., Freemont, A.J., and Hoyland, J.A. (2007). Accelerated cellular senescence in degenerate intervertebral discs: a possible role in the pathogenesis of intervertebral disc degeneration. Arthritis Res. Ther. *9*, R45.

Lee, D.C., Adams, C.S., Albert, T.J., Shapiro, I.M., Evans, S.M., and Koch, C.J. (2007). In situ oxygen utilization in the rat intervertebral disc. J. Anat. *210*, 294–303.

Li, F.C., Zhang, N., Chen, W.S., and Chen, Q.X. (2010). Endplate degeneration may be the origination of the vacuum phenomenon in intervertebral discs. Med. Hypotheses *75*, 169–171.

Liu, L.T., Huang, B., Li, C.Q., Zhuang, Y., Wang, J., and Zhou, Y. (2011). Characteristics of stem cells derived from the degenerated human intervertebral disc cartilage endplate. PLoS One *6*, e26285.

Lue, H., Kleemann, R., Calandra, T., Roger, T., and Bernhagen, J. (2002). Macrophage migration inhibitory factor (MIF): mechanisms of action and role in disease. Microbes Infect. *4*, 449–460.

Maity, A., and Koumenis, C. (2006). HIF and MIF—a nifty way to delay senescence? Genes Dev. *20*, 3337–3341.

Markert, J.M., Fuller, C.M., Gillespie, G.Y., Bubien, J.K., McLean, L.A., Hong, R.L., Lee, K., Gullans, S.R., Mapstone, T.B., and Benos, D.J. (2001). Differential gene expression profiling in human brain tumors. Physiol. Genomics *5*, 21–33.

Martin-Rendon, E., Hale, S.J., Ryan, D., Baban, D., Forde, S.P., Roubelakis, M., Sweeney, D., Moukayed, M., Harris, A.L., Davies, K., et al. (2007). Transcriptional profiling of human cord blood CD133+ and cultured bone marrow mesenchymal stem cells in response to hypoxia. Stem Cells *25*, 1003–1012.

Merceron, C., Vinatier, C., Portron, S., Masson, M., Amiaud, J., Guigand, L., Cherel, Y., Weiss, P., and Guicheux, J. (2010). Differential effects of hypoxia on osteochondrogenic potential of human adipose-derived stem cells. Am. J. Physiol. Cell Physiol. *298*, C355–C364.

Nerlich, A.G., Schaaf, R., Walchli, B., and Boos, N. (2007). Temporo-spatial distribution of blood vessels in human lumbar intervertebral discs. Eur. Spine J. *16*, 547–555.

Ohta, S., Misawa, A., Lefebvre, V., Okano, H., Kawakami, Y., and Toda, M. (2013). Sox6 up-regulation by macrophage migration inhibitory factor promotes survival and maintenance of mouse neural stem/progenitor cells. PLoS One *8*, e74315.

Onodera, S., Nishihira, J., Iwabuchi, K., Koyama, Y., Yoshida, K., Tanaka, S., and Minami, A. (2002). Macrophage migration inhibitory factor up-regulates matrix metalloproteinase-9 and -13 in rat osteoblasts. Relevance to intracellular signaling pathways. J. Biol. Chem. *277*, 7865–7874.

Onodera, S., Sasaki, S., Ohshima, S., Amizuka, N., Li, M., Udagawa, N., Irie, K., Nishihira, J., Koyama, Y., Shiraishi, A., et al. (2006). Transgenic mice overexpressing macrophage migration inhibitory factor (MIF) exhibit high-turnover osteoporosis. J. Bone Miner. Res. *21*, 876–885.

Peng, B., Hao, J., Hou, S., Wu, W., Jiang, D., Fu, X., and Yang, Y. (2006). Possible pathogenesis of painful intervertebral disc degeneration. Spine (Phila Pa 1976) *31*, 560–566.

Petrenko, O., and Moll, U.M. (2005). Macrophage migration inhibitory factor MIF interferes with the Rb-E2F pathway. Mol. Cell *17*, 225–236.

Petrenko, O., Fingerle-Rowson, G., Peng, T., Mitchell, R.A., and Metz, C.N. (2003). Macrophage migration inhibitory factor deficiency is associated with altered cell growth and reduced susceptibility to Ras-mediated transformation. J. Biol. Chem. *278*, 11078–11085.

Pfirrmann, C.W., Metzdorf, A., Zanetti, M., Hodler, J., and Boos, N. (2001). Magnetic resonance classification of lumbar intervertebral disc degeneration. Spine (Phila Pa 1976) *26*, 1873–1878.

Piera-Velazquez, S., Hawkins, D.F., Whitecavage, M.K., Colter, D.C., Stokes, D.G., and Jimenez, S.A. (2007). Regulation of the human SOX9 promoter by Sp1 and CREB. Exp. Cell Res. *313*, 1069–1079.

Pyle, M.E., Korbonits, M., Gueorguiev, M., Jordan, S., Kola, B., Morris, D.G., Meinhardt, A., Powell, M.P., Claret, F.X., Zhang, Q., et al. (2003). Macrophage migration inhibitory factor expression is

increased in pituitary adenoma cell nuclei. J. Endocrinol. *176*, 103–110.

Raj, P.P. (2008). Intervertebral disc: anatomy-physiology-pathophysiology-treatment. Pain Pract. *8*, 18–44.

Rajpurohit, R., Risbud, M.V., Ducheyne, P., Vresilovic, E.J., and Shapiro, I.M. (2002). Phenotypic characteristics of the nucleus pulposus: expression of hypoxia inducing factor-1, glucose transporter-1 and MMP-2. Cell Tissue Res. *308*, 401–407.

Redshaw, Z., and Loughna, P.T. (2012). Oxygen concentration modulates the differentiation of muscle stem cells toward myogenic and adipogenic fates. Differentiation *84*, 193–202.

Roberts, S., Urban, J.P., Evans, H., and Eisenstein, S.M. (1996). Transport properties of the human cartilage endplate in relation to its composition and calcification. Spine (Phila Pa 1976) *21*, 415–420.

Robins, J.C., Akeno, N., Mukherjee, A., Dalal, R.R., Aronow, B.J., Koopman, P., and Clemens, T.L. (2005). Hypoxia induces chondrocyte-specific gene expression in mesenchymal cells in association with transcriptional activation of Sox9. Bone *37*, 313–322.

Schiller, Z.A., Schiele, N.R., Sims, J.K., Lee, K., and Kuo, C.K. (2013). Adipogenesis of adipose-derived stem cells may be regulated via the cytoskeleton at physiological oxygen levels in vitro. Stem Cell Res. Ther. *4*, 79.

Semenza, G.L. (2001). Hypoxia-inducible factor 1: oxygen homeostasis and disease pathophysiology. Trends Mol. Med. *7*, 345–350.

Tamiya, H., Ikeda, T., Jeong, J.H., Saito, T., Yano, F., Jung, Y.K., Ohba, S., Kawaguchi, H., Chung, U.I., and Choi, J.Y. (2008). Analysis of the Runx2 promoter in osseous and non-osseous cells and identification of HIF2A as a potent transcription activator. Gene *416*, 53–60.

Taylor, J.R., Kuchel, G.A., Hegde, P., Voznesensky, O.S., Claffey, K., Tsimikas, J., Leng, L., Bucala, R., and Pilbeam, C. (2007). Null mutation for macrophage migration inhibitory factor (MIF) is associated with less aggressive bladder cancer in mice. BMC Cancer *7*, 135.

Wagegg, M., Gaber, T., Lohanatha, F.L., Hahne, M., Strehl, C., Fangradt, M., Tran, C.L., Schonbeck, K., Hoff, P., Ode, A., et al. (2012). Hypoxia promotes osteogenesis but suppresses adipogenesis of human mesenchymal stromal cells in a hypoxia-inducible factor-1 dependent manner. PLoS One *7*, e46483.

Walsh, D.A., McWilliams, D.F., Turley, M.J., Dixon, M.R., Franses, R.E., Mapp, P.I., and Wilson, D. (2010). Angiogenesis and nerve growth factor at the osteochondral junction in rheumatoid arthritis and osteoarthritis. Rheumatology (Oxford) *49*, 1852–1861.

Wang, A.M., Cao, P., Yee, A., Chan, D., and Wu, E.X. (2015). Detection of extracellular matrix degradation in intervertebral disc degeneration by diffusion magnetic resonance spectroscopy. Magn. Reson. Med. *73*, 1703–1712.

Winner, M., Koong, A.C., Rendon, B.E., Zundel, W., and Mitchell, R.A. (2007). Amplification of tumor hypoxic responses by macrophage migration inhibitory factor-dependent hypoxia-inducible factor stabilization. Cancer Res. *67*, 186–193.

Xiong, C., Huang, B., Cun, Y., Aghdasi, B.G., and Zhou, Y. (2014). Migration inhibitory factor enhances inflammation via CD74 in cartilage end plates with Modic type 1 changes on MRI. Clin. Orthop. Relat. Res. *472*, 1943–1954.

Xuan, N.T., Choi, J.W., Lee, S.B., Ye, K., Woo, S.D., Lee, K.H., and Ahn, J.Y. (2006). Akt phosphorylation is essential for nuclear translocation and retention in NGF-stimulated PC12 cells. Biochem. Biophys. Res. Commun. *349*, 789–798.

Yang, D.C., Yang, M.H., Tsai, C.C., Huang, T.F., Chen, Y.H., and Hung, S.C. (2011). Hypoxia inhibits osteogenesis in human mesenchymal stem cells through direct regulation of RUNX2 by TWIST. PLoS One *6*, e23965.

Zhang, Y., Hassan, M.Q., Xie, R.L., Hawse, J.R., Spelsberg, T.C., Montecino, M., Stein, J.L., Lian, J.B., van Wijnen, A.J., and Stein, G.S. (2009). Co-stimulation of the bone-related Runx2 P1 promoter in mesenchymal cells by SP1 and ETS transcription factors at polymorphic purine-rich DNA sequences (Y-repeats). J. Biol. Chem. *284*, 3125–3135.

Zhang, Q.B., Zhang, Z.Q., Fang, S.L., Liu, Y.R., Jiang, G., and Li, K.F. (2014). Effects of hypoxia on proliferation and osteogenic differentiation of periodontal ligament stem cells: an in vitro and in vivo study. Genet. Mol. Res. *13*, 10204–10214.